

TOPICAL REVIEW

Recent progress in mesoporous titania materials: adjusting morphology for innovative applications

Juan L Vivero-Escoto¹, Ya-Dong Chiang², Kevin C-W Wu^{2,3}
and Yusuke Yamauchi^{4,5,6}

¹ Department of Chemistry, The University of North Carolina at Chapel Hill, Chapel Hill, NC 27599, USA

² Department of Chemical Engineering, National Taiwan University, No. 1, Sec. 4, Roosevelt Road, Taipei 10617, Taiwan

³ Division of Medical Engineering Research, National Health Research Institutes, 35 Keyan Road, Zhunan, Miaoli County 350, Taiwan

⁴ World Premier International (WPI) Research Center for Materials Nanoarchitectonics (MANA), National Institute for Materials Science (NIMS), 1-1 Namiki, Tsukuba, Ibaraki 305-0044, Japan

⁵ Faculty of Science and Engineering Waseda University, 3-4-1 Okubo, Shinjuku, Tokyo 169-8555, Japan

⁶ Precursory Research for Embryonic Science and Technology (PRESTO), Japan Science and Technology Agency (JST), 4-1-8 Honcho, Kawaguchi, Saitama 332-0012, Japan

E-mail: kevinwu@ntu.edu.tw and Yamauchi.Yusuke@nims.go.jp

Received 2 August 2011

Accepted for publication 18 August 2011

Published 2 February 2012

Online at stacks.iop.org/STAM/13/013003

Abstract

This review article summarizes recent developments in mesoporous titania materials, particularly in the fields of morphology control and applications. We first briefly introduce the history of mesoporous titania materials and then review several synthesis approaches. Currently, mesoporous titania nanoparticles (MTNs) have attracted much attention in various fields, such as medicine, catalysis, separation and optics. Compared with bulk mesoporous titania materials, which are above a micrometer in size, nanometer-sized MTNs have additional properties, such as fast mass transport, strong adhesion to substrates and good dispersion in solution. However, it has generally been known that the successful synthesis of MTNs is very difficult owing to the rapid hydrolysis of titanium-containing precursors and the crystallization of titania upon thermal treatment. Finally, we review four emerging fields including photocatalysis, photovoltaic devices, sensing and biomedical applications of mesoporous titania materials. Because of its high surface area, controlled porous structure, suitable morphology and semiconducting behavior, mesoporous titania is expected to be used in innovative applications.

Keywords: mesoporous material, mesoporous titania, nanoparticle, photocatalyst, solar cell

1. Introduction

The International Union of Pure and Applied Chemistry (IUPAC) classifies porous materials into three types depending on their pore sizes: microporous materials with pore sizes below 2 nm, mesoporous materials with pore

sizes between 2 and 50 nm, and macroporous materials with pore sizes larger than 50 nm [1–3]. Mesoporous materials exhibit several geometric mesostructures (lamellar, two-dimensional (2D) hexagonal, three-dimensional (3D) hexagonal and cubic), morphologies (powder, nanoparticles and film), and framework compositions (inorganics, organics,

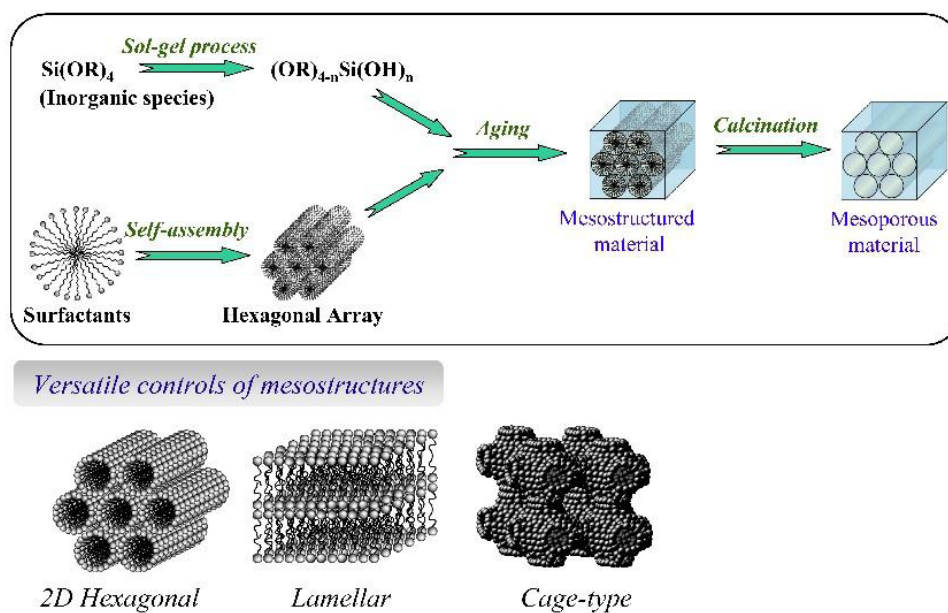


Figure 1. Synthesis pathway for formation of mesoporous silica materials. Several geometric mesostructures (e.g. 2D hexagonal, lamellar and cage-type) can be produced by varying the synthesis conditions.

metals and metal oxides; figure 1). Various applications have been proposed for each mesoporous material. Mesoporous materials are widely used as hosts because they are capable of encapsulating bulky molecules into mesopores that cannot be achieved using microporous materials, such as zeolites. In addition, mesoporous materials have a high surface area, uniform and tunable pore sizes, and various morphologies and compositions, which favor their applications in various fields including environmental energy, optics, medicine, electronics and biotechnology.

Since the first synthesis of the FSM and M41S families in 1990s by Kuroda *et al.* in Japan [4] and the Mobil Oil Corporation in USA [5], mesoporous ‘silica’ materials have been widely investigated. In the meantime, mesoporous ‘transition metal oxides’ have also attracted much attention because they exhibit both intrinsic optical and electronic properties of transition metal oxides and the advantages of mesopores [6–9]. Among mesoporous transition metal oxides, mesoporous titania (TiO_2) is one of the most intensively studied materials owing to its versatile applications.

In the mid-1990s, Antonelli and Ying synthesized the first mesoporous TiO_2 powder with a highly organized hexagonal pore structure by combining the phosphate surfactant templating chemistry with a modified sol–gel process [10]. Since then, similar approaches with various titanium sources or templating surfactants have also been presented for the synthesis of ordered mesostructured (template was preserved) or mesoporous (template was removed) TiO_2 with diverse morphologies [11–13].

The high performance of mesoporous titania in photocatalysis and optical devices has been known since the early 20th century. Mesoporous titania materials are expected to play an important role in solving environmental and pollution challenges and easing the energy crisis through the effective utilization of solar energy based on photovoltaic

devices. Some of the attractive features of mesoporous titania nanoparticles (MTNs) are their high surface area, pore size, larger pore volume and ordered porous structure, which result in a high density of reactive sites and an efficient mass transport. In this review, we focus on the preparation methods, morphology control and applications of mesoporous titania materials.

2. Synthesis methods

2.1. Mesoporous titania bulks

Similarly to the synthesis of mesoporous silica, the synthesis of mesoporous titania also requires a surfactant as a structure-directing agent and a material source. However, different from silica, titania sources, such as titanium alkoxides and titanium tetrachloride, usually undergo very rapid hydrolysis and condensation, resulting in the precipitation of TiO_2 without the formation of mesopores. Therefore, a careful control of synthesis conditions is critical. For instance, Ulagappan and Rao successfully prepared 2D hexagonal mesoporous TiO_2 using neutral amine surfactants and $\text{Ti}(\text{OPr})_4$ as a titanium source [11]. Froba *et al.* attempted to use three different bidentate ligands (1,3-propanediol, 1,5-pentanediol and 2,4-pentanedione) to modify the reactivity of titanium tetraisopropoxide and obtain ordered mesostructured TiO_2 [12]. Niessen *et al.* prepared Ti-based MCM-41 materials using $(\text{NH}_4)_3[\text{Ti}(\text{O}_2)\text{F}_5]$ as a novel titanium source [13]. They also compared the effects of different surfactants with dissimilar chain lengths to vary the pore sizes from 16 to 27 nm.

In 1999, Antonelli proposed a phosphorous-free synthesis method for mesoporous titania that combined amine surfactants and dry aging [14]. The phosphorous originating from the templating surfactants is difficult to remove

by either calcination or solvent extraction [10]. This drawback limits the possible uses of phosphorous-containing mesoporous titania as a catalyst or catalyst support. Therefore, the phosphorous-free synthesis method is very important for mesoporous pure titania materials. The preparation of mesostructured phosphorous-free titanium oxide in the presence of Na^+ and TMA^+ (tetramethyl ammonium hydroxide) using a cationic surfactant (CTABr) as a structure-directing agent and soluble peroxytitanate as a precursor, respectively, was also reported [15]. Yang *et al* described the synthesis of thermally stable and large-pore mesoporous metal oxides using block copolymers as structure-directing agents [16]. Zheng *et al* synthesized mesoporous titania with a mixture of organic compounds as a non-surfactant template [17]. However, the complexity of the phosphorous-free synthesis of mesoporous titania urged researchers to seek facile and time-saving methods for preparing well-crystallized mesoporous titania materials.

2.2. Mesoporous titania films

Over the last decade, a number of synthesis procedures for mesoporous titania films have been developed by different groups, and several recent papers have focused on the effects of the aging condition, the pH of the precursor solution, and the calcination temperature on the mesostructural ordering. The most convenient method of preparing mesoporous titania films is solvent evaporation, which was first proposed by Ogawa [18,19]. Through the coating of precursor solutions, which include ethanol, inorganic species and surfactants, mesoporous titania films with various mesostructures, such as lamellar and 2D hexagonal mesostructures, can be prepared [20–24]. Yun *et al* reported the first example of anatase-crystallized mesoporous titania thin films with a 2D hexagonal mesoporous structure using the solvent evaporation method (figure 2(a)) [20]. Smarsly *et al* also applied the solvent evaporation method to fabricate highly organized mesoporous anatase films by the hydrolysis/condensation of TiCl_4 in the presence of polyhydroxybutyrate-(polyethylene oxide) block copolymer templates [22]. The solvent evaporation method, which is commonly called the evaporation-induced self-assembly (EISA) method, is employed to rapidly produce mesoporous titania films. In most cases, TiCl_4 was chosen as a titanium source, but the control of the hydrolysis is more difficult for TiCl_4 than for other titanium sources. In addition, the pH of the precursor solution is reduced to very low values after the addition of TiCl_4 . Titanium tetraisopropoxide (TTIP) is an alternative titanium source which results in a high reproducibility of the synthesis and is easy to handle. Wu *et al* found that the low aging temperature slowed down the hydrolysis and condensation reactions of TTIP that favored the formation of a highly ordered structure (figures 2(b) and (c)) [23]. Very recently, Nilsson *et al* developed a new direct synthesis methodology by using a microemulsion route for the preparation of mesoporous titania films with a 2D hexagonal mesostructure [24]. The crystallinity and crystallite size in the pore walls were controlled within an acceptable range at

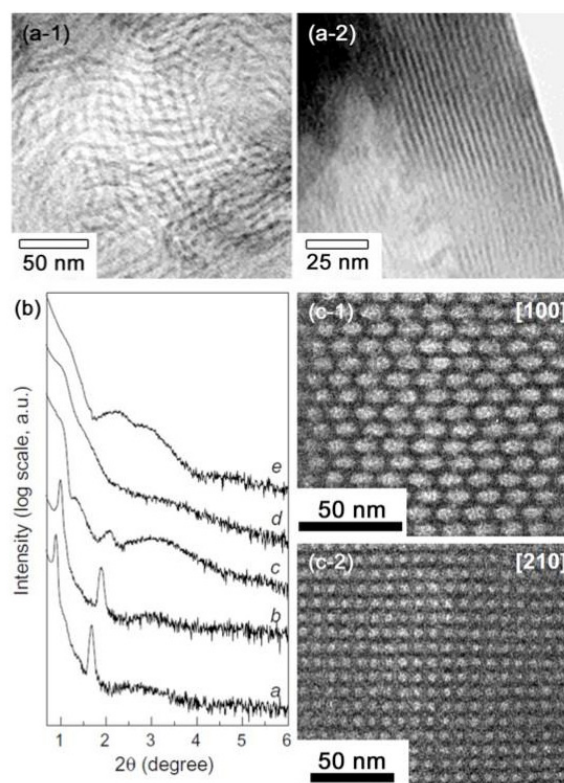


Figure 2. (a) Transmission electron microscopy (TEM) images of mesoporous titania films with 2D hexagonal mesostructure (reprinted with permission from [20] ©2001 John Wiley and Sons Inc.). (b) Low-angle x-ray diffraction patterns of P123-templated mesoporous titania thin films aged at -20°C (trace a), 2°C (trace b), 25°C (trace c), 60°C (trace d), and 90°C (trace e). (c) Cross-sectional TEM images of P123-templated mesoporous titania thin films ($P6_3/mmc$) aged at -20°C .

40°C without the need for an autoclave or high-temperature post-treatment procedures, which makes this technique very interesting for crystal engineering with mesoporous materials.

2.3. Hierarchical mesoporous titania

Recently, titanium materials with a hierarchical structure have also attracted some interest. Carbajo *et al* prepared a hierarchically 3D-ordered meso- and macro-porous titania material using arrays of latex particles with different compositions as templates and titanium tetraisopropoxide as the precursor [25]. Ma *et al* synthesized hierarchically meso- and macro-porous titanium tetraphosphonate materials with ethylenediamine groups within the framework by a simple surfactant-free process in a very wide pH range of 3–13 [26]. They found that pH strongly affected the morphology and texture of the resultant titanium phosphonate materials.

2.4. Mesoporous titania nanoparticles (MTNs)

Before the discovery of MTNs, several types of titania nanoparticles lacking a mesoporous structure were widely synthesized. In 2000, Wang *et al* prepared well-defined TiO_2 spheres using a titanium tetraisopropoxide ($\text{Ti}(\text{OPr})_4$)

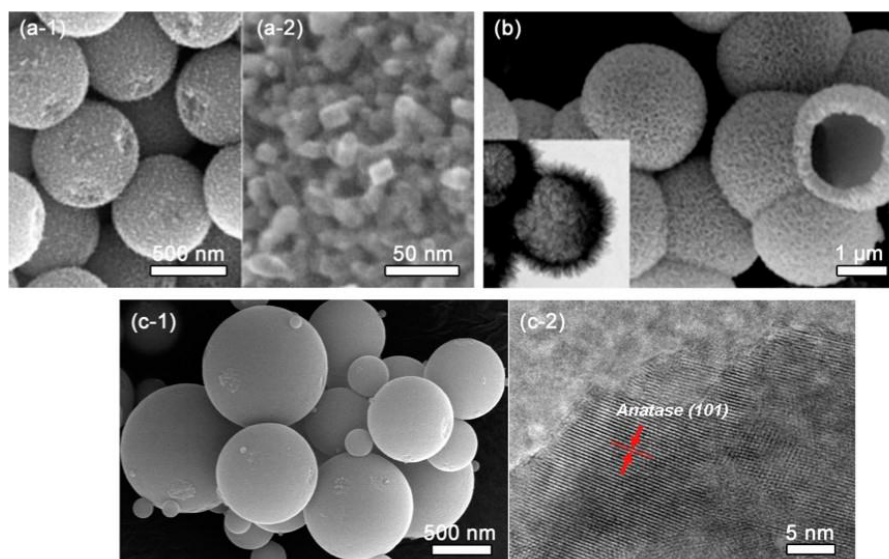


Figure 3. (a) Scanning electron microscopy (SEM) images of the calcined mesoporous titania beads obtained with solvothermal process (reprinted with permission from [34] ©2009 John Wiley and Sons Inc.). (b) SEM and TEM images of mesoporous titania hollow spheres (reprinted with permission from [39] ©2007 American Chemical Society). (c) SEM and TEM images of mesoporous titania spheres prepared by spray drying (reprinted with permission from [50]).

precursor under static conditions [27]. Han *et al* synthesized highly crystalline TiO₂ nanocrystals with various shapes and crystal structures via controlled sol–gel reactions in aqueous media without further hydrothermal treatment [28]. Shibata *et al* directly synthesized crystalline titania particles by varying temperature and reaction time in the sol–gel reaction process [29]. Choi *et al* investigated the effects of the type and concentration of surfactant (e.g. T20, T80 and X100) on the homogeneity, morphology, light absorption, dye adsorption and degradation, and hydrophilicity of TiO₂ particles [30]. Hafez synthesized highly active single-crystal TiO₂ nanorods via a simple two-step hydrothermal method [31]. Tanaka *et al* prepared monodispersed titania spheres with a diameter in the range of 380–960 nm by the hydrolysis and condensation of titanium tetraisopropoxide. They used ammonia or dodecylamine as a catalyst in a methanol/acetonitrile co-solvent at room temperature [32]. More facile and direct methods to synthesize titania nanoparticles have appeared recently, providing numerous benefits to applications. The lack of pores in the nanoparticles usually results in a low surface area. Consequently, many researchers focus on the synthesis of titanium nanoparticles with mesopores (namely, MTNs). These materials should be of interest in various fields, such as sensing, photoelectric devices and biotechnology.

MTNs have been widely studied in recent years. In 2007, Kim and Kwak synthesized MTNs by hydrothermal treatment [33]. They found that hydrothermal treatment significantly affects the physical properties of meso- and macro-porous TiO₂, particularly crystal composition, crystallinity, thermal stability, surface area, pore size distribution and photocatalytic activity. The Caruso group reported the synthesis of crystalline, mesoporous TiO₂ beads with surface areas up to 108.0 m² g⁻¹ and tunable pore sizes (14.0–22.6 nm) through a facile combination of sol-gel and solvothermal processes (figure 3(a)) [34]. In 2010,

Guo *et al* fabricated two types of 3D mesoporous TiO₂ microspheres using various titanium sources via a one-step solvothermal process without templates [35]. Sun *et al* reported a facile hydrolysis method for the synthesis of spherical MTNs using titanium tetrachloride under mild conditions [36]. They systematically investigated the effects of reaction conditions, such as Ti⁴⁺ ion concentration and water content, on the formation of MTNs. The Caruso group prepared monodispersed mesoporous anatase titania beads with a high surface area and a tunable pore size through a combined sol–gel and solvothermal process in the presence of hexadecylamine as a structure-directing agent [37]. Wang *et al* prepared mesoporous titania spheres with a high monodispersity by employing monodispersed poly(styrene-co-methacrylic acid) (PSMAA) particles. The spheres had an average diameter of about 130 nm and a pore size of about 4 nm [38]. Hollow titania spheres are another interesting MTN morphology [39, 40]. In 2007, Li *et al* synthesized hollow titania spheres with a unique urchin-like shape and a tunable interior structure (figure 3(b)) [39], and Ye *et al* prepared TiO₂ hollow microspheres with an average external diameter of 1.75 μm by a simple hydrothermal method [40].

The synthesis of MTNs can be assisted by ultrasound. Wang *et al* prepared MTNs with a high surface area using ultrasonication, completing the process within a few hours [41]. Mesostructured TiO₂ was obtained with ultrasound irradiation, using octadecylamine as the structure-directing agent and Ti(OPr)₄ as the precursor. Yu *et al* synthesized mesoporous TiO₂ without using any surfactant by intense ultrasound irradiation for a short time [42]. Monodispersed TiO₂ sol particles were formed initially by the ultrasound-assisted hydrolysis of titanium tetraisopropoxide modified with acetic acid. Then, the mesoporous particles were produced by the controlled

condensation and agglomeration of the sol nanoparticles under intense ultrasound irradiation.

Spray drying is a facile, reproducible and scalable technology for the fabrication of mesoporous particles [43–49]. During this process, a precursor solution consisting of inorganic species, surfactants and solvents is sprayed through a nozzle into a hot chamber with the aid of a gas stream. The evaporation-induced self-assembly of droplets is the main mechanism to create mesoporous particles. Since its first report in 1999 [43], this process has been used to fabricate mesoporous particles with different sizes, internal structures and compositions, including silica, organosilica, carbon, and metal oxides [44–49]. Oveisi *et al* proposed a facile, reproducible and scalable spray-drying synthesis method for mesoporous titania spheres (figure 3(c)) [50]. Their size and crystal phases (anatase and rutile) were changed by varying the calcination temperature [50]. The surface areas and pore volume were reduced by increasing the calcination temperature from 350 to 700 °C, while the average pore diameter was increased. This is due to the distortion of the mesostructure by the grain growth of the anatase phase and further transformation to the rutile phase during the calcination process. The mesoporous titania particles calcined at 400 °C exhibited both a high surface area and a well-developed anatase phase, thereby showing the highest photocatalytic activity.

3. Applications

Since the beginning of the last century, TiO₂ materials have been extensively used in sunscreens, paints, ointments and toothpaste. Later on, the phenomenon of photocatalytic splitting of water on a TiO₂ electrode under UV light was discovered. Since then, much effort has been devoted to the development and application of TiO₂ materials in photovoltaics, photocatalysis, photo-electrochromics and sensors [51].

3.1. Photocatalysis

TiO₂ is known as the most efficient and environmentally friendly photocatalyst. The principle of TiO₂ photocatalytic properties is straightforward [52–54]. Upon the absorption of light with an energy larger than the band gap of TiO₂, electrons are excited from the valence band to the conduction band, creating electron-hole (e⁻-h⁺) pairs. These e⁻-h⁺ pairs migrate to the surface and react with the chemicals adsorbed there. This photocatalytic process usually involves one or more radicals or intermediate species, such as OH, O₂⁻, H₂O₂, or O₂, which play an important role in the photodecomposition. Surface area and crystallinity affect the photocatalytic efficiency of mesoporous TiO₂ materials: a larger surface area increases the reaction rate, whereas the presence of amorphous phases promotes e⁻-h⁺ recombination, thereby decreasing photocatalytic activity.

Surfactants, triblock copolymer and many organic compounds have been used to prepare mesoporous TiO₂. Solvent extraction or thermal treatment was then applied

to remove the surfactants used in the preparation process. The photocatalytic activity of the obtained amorphous TiO₂ is usually insignificant. However, calcination at a high temperature results in the collapse of the mesoporous framework and the reduction in surface area because of the crystallization of TiO₂. For this reason, it is still a challenge to synthesize mesoporous TiO₂ materials containing highly crystalline anatase walls and a large surface area.

To overcome this issue, Linden *et al* have used protons in acid media to slow down the condensation [55]. Peng *et al* have reported a hydrothermal synthesis method for anatase MTNs using cetyl trimethylammonium bromide (CTAB) as a surfactant-directing and pore-forming agent [56]. The particles had a high surface area and a uniform mesopore. They showed a very high photocatalytic activity to the oxidation of Rhodamine B, exceeding that of the commercial catalyst Degussa P25: 97% of Rhodamine B was degraded within 2 h with the MTNs, and only 60% with Degussa P25. To further enhance the photocatalytic properties of these nanoparticles, the authors doped them with lanthanum ions [57] and achieved an even higher photocatalytic activity than with the undoped MTNs. This high photocatalytic activity is related to the large surface area, as well as the high density of active sites for combining with organic compounds induced by the lanthanum ions in the MSN framework. Following the same strategy, these authors also prepared cerium-doped MTNs [58] and observed an increase in surface area and thermal stability. However, while the cerium-doped MTNs exhibited a higher photocatalytic activity than P25, the maximum degradation rate of Rhodamine B was obtained with the undoped sample. This result was attributed to cerium partially blocking the active sites available for photodegradation. Recently, Dai *et al* have used the La-doped MTNs for environmental purposes. The authors addressed the degradation of phoxim, an organophosphorus pesticide with a high toxicity for biotic systems [59].

As mentioned above, the photocatalytic activity can be improved by increasing the crystallinity of the material. This can be achieved with a high-temperature treatment; however, the annealing of typical mesoporous TiO₂ usually leads to an undesirable grain growth and a total collapse of the ordered mesoporous network. To overcome this problem, various metals have been used as dopants to increase the thermal stability of mesoporous titania, i.e. to prevent the rapid growth of anatase crystals in the framework [60–63]. Zhou *et al* recently have reported a combination of an evaporation-induced self-assembly (EISA) with encircling ethylenediamine (EN) protectors and prepared thermally stable (above 700 °C) ordered mesoporous anatase TiO₂ with a high crystallinity, a large surface area and a large pore size (10 nm) [64]. The authors successfully tested the photocatalytic activity of this TiO₂ material for the degradation of highly toxic 2,4-dichlorophenol under UV irradiation. Oveisi *et al* also reported an outstanding antibacterial property of mesoporous anatase films prepared by the calcination of ordered mesoporous titania films (figure 4) [65, 66].

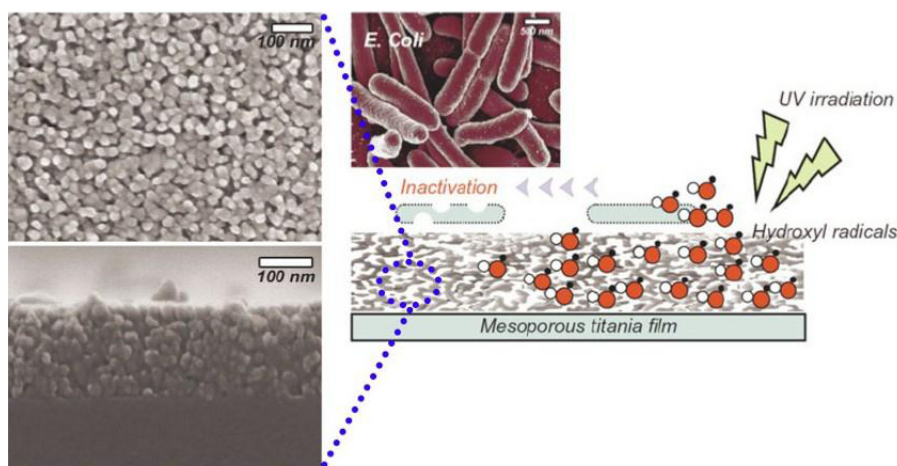


Figure 4. Schematic of inactivation of *Escherichia coli* (*E. coli*) on surface of mesoporous titania film during UV irradiation. The top-center panel shows an SEM image of *E. coli* (copyright-free image from homepage of ‘National Institute of Allergy and Infectious Diseases (NIAID)’). The two left panels show the SEM images of the top layers of the calcined mesoporous titania films (reprinted with permission from [66] ©2010 John Wiley and Sons Inc.).

3.2. Photovoltaic applications

The marked increase in energy demand and the challenges of climate change have urged the development of alternative energy and sustainable environmental technologies. In addition, with the depletion of fossil fuels, it has become evident that environment-friendly energy sources should be used to create, transport and produce electricity from natural resources [67]. Dye-sensitized solar cells (DSSCs) are a promising substitute. Their action is based on the photoexcitation of dye molecules adsorbed on the surface of a thin film of a semiconductor, such as titania or ZnO nanomaterials acting as an anode electrode [68–71]. DSSCs contain three main parts: the dye-sensitized semiconducting nanocrystalline film acting as the photoanode, the redox couple (usually I_3^-/I^-) in organic solvent(s), and the platinized transparent conducting oxide (TCO) glass as the counter electrode. The main part of the system is a nanocrystalline mesoporous TiO_2 film with a monolayer of the charge-transfer dye attached to its surface. The film is placed in a redox electrolyte (I_3^-/I^-). The photoexcitation of the dye injects electrons into the conduction band of TiO_2 , which can be conducted to the outer circuit to generate electric power. The dye molecules can be regenerated by the iodide ions in the electrolyte, and then the resulting triiodide ions can accept electrons from the platinized TCO counter electrode to complete the current cycle in a DSSC. Generally, the device generates electric power from light without undergoing any permanent chemical transformation.

TiO_2 is one of the most popular materials used in the porous film electrode of DSSCs, and its particle size and shape are crucial for the photoelectric conversion efficiency of DSSCs [72]. TiO_2 materials with different shapes, such as nanoparticles, nanotubes, nanowires and nanofibers, have been applied to fabricate the porous film electrodes [73–75]. It is expected that the large surface area and pore volume of MTNs will improve the dye absorption, thereby increasing the light absorption efficiency in DSSCs. To prove this idea,

Khan *et al* synthesized nanocrystalline mesoporous titania of the anatase crystal phase for DSSC applications [76]. Its Brunauer–Emmett–Teller (BET) surface area and pore size were $80.1\text{ m}^2\text{ g}^{-1}$ and 2.7 nm, respectively. Films prepared from these MTNs were used as working electrodes for DSSCs, which were compared with the cells based on the commercially available P-25 (Degussa) nanoparticles. The authors obtained a fill factor of 51.12% with an energy conversion efficiency of 7.59% under 1 sun irradiation in the optimized mesoporous substrate used in the fabrication of DSSCs. They demonstrated that the surface area of MTNs affects the conversion efficiency of the DSSCs.

Zhao *et al* also synthesized MTNs for the fabrication of porous film electrodes. They evaluated the effects of the annealing temperature of porous electrodes on the photoelectrochemical properties of DSSCs [77] and found an optimum at 500 °C. The authors examined the kinetic processes in DSSCs using the electrical impedance spectroscopy and open-circuit voltage decay curves, and found that the bulk traps and the surface states within the porous electrodes affect the recombination reaction, and therefore the short-circuit current (I_{sc}) and open-circuit photovoltage (V_{oc}) of DSSCs. The mesostructures within the MTNs also improve the dye adsorption and thus the photoelectrochemical properties of DSSCs. The highest photoelectric conversion efficiency (10.12%) was measured for the DSSCs fabricated with MTNs; it was 3.79% higher than that of the P25-based DSSC. However, these mesoporous film-based solar cells lack depletion layers at the electrode/dye/electrolyte interfaces [78]. Therefore, the back electron transfer (i.e. charge recombination) at the interfaces still remains a major limiting factor for enhancing the cell performance. To overcome this issue, the surface of MTNs is coated with different materials, such as SiO_2 , Al_2O_3 and ZrO_2 . Peng *et al* modified the surface of MTNs with $Mg(NO_3)_2$ solution through dipping followed by annealing [79]. They studied the effects of the Mg^{2+} concentration on the surface states and charge recombination of the MTN electrode on the

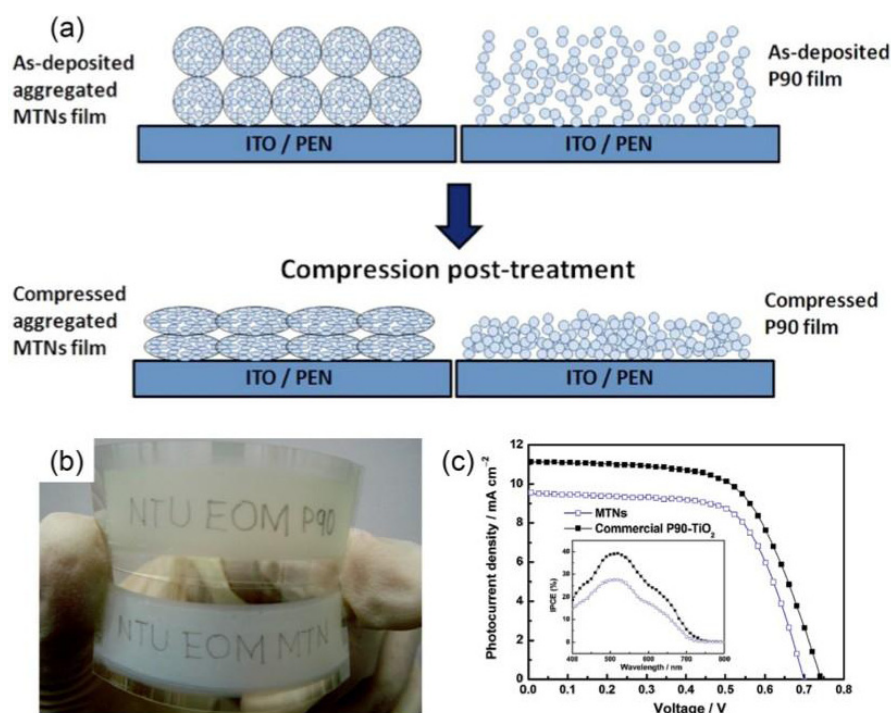


Figure 5. (a) Schematic of electrophoretic deposition of MTN and P90 films and the subsequent compression post-treatment. (b) Photograph of bent P90 (top) and MTN (bottom) films after compression at 100 MPa with HB pencil writing. (c) J - V curves of MTN-based and P90-based DSSCs with thickness of 11 μm measured under 100 mW cm^{-2} illumination. The inset shows the incident-photon-to-electron conversion efficiency spectra (reprinted with permission from [81] ©2011 RSC Publishing).

solar cell efficiency. The optimal efficiency was obtained for the MTN electrode modified with 0.2 MMg^{2+} solution, which was 39% higher than that in the unmodified electrode.

Different approaches have been developed to further enhance the photo-electrochemical performance of MTNs. For example, Patra *et al* observed the self-assembly of small MTNs when sodium salicylate was used as a template [80]. They also observed a significant enhancement of the photoelectrochemical response of MTNs under visible light irradiation after photosensitizer molecules (dye) were entrapped inside the mesopores. The authors projected that the efficient synthesis strategy and enhanced photoresponse of these mesoporous TiO₂ materials could facilitate the design of other porous semiconductor oxides and their applications in photon-to-electron conversion processes.

Flexible DSSCs are considered as another type of DSSCs that are handy and convenient for transportation. In particular, flexible DSSCs using thin and lightweight conducting plastic substrates as their photoelectrodes are cheap and suitable for roll-to-roll production. However, one critical problem that has restricted the development of plastic-based DSSCs is that the plastic substrate cannot be subjected to a high sintering temperature (450–550 °C) for improving the attachment of the TiO₂ particles to the substrate. Chen *et al* reported an electrophoretic deposition of MTNs as an alternative to the commercial TiO₂ particles (P90) and used the deposited MTN film as a photoelectrode for plastic DSSCs (figure 5). The synthesized MTNs with an average size of around 260 nm consist of primary anatase nanocrystallites (about 12.5 nm) and show fewer grain boundaries and defects, and higher

dye-adsorption and light scattering than commercial P90 TiO₂ particles. Consequently, the MTN-based plastic DSSCs exhibited an excellent conversion efficiency of 5.25%, which was 1% higher than that of the cell containing P90 TiO₂ particles [81].

3.3. Sensing applications

Mesoporous titania has recently been studied for gas sensor applications. For example, Devi *et al* found that ordered mesoporous TiO₂ exhibited higher H₂ and CO sensitivities than sensors fabricated from common TiO₂ powders owing to the increased surface area [82]. The sensitivity could be further improved by loading the sensor with 0.5 mol% of Nb₂O₅. Benkstein and Semancik found that mesoporous TiO₂ film platforms could be used as high-sensitivity conductometric gas sensor materials [83]. They attributed the high sensitivity to the large internal surface area in the mesoporous films.

3.4. Biomedical applications

Despite the growing interest and application of mesoporous TiO₂ materials in a wide variety of fields, little has been published on their biomedical applications. One reason for this could be that the preparation of nanostructured mesoporous titania materials is not trivial. Recently, Wu *et al* have reported the synthesis, characterization and biomedical application of MTNs (figure 6) [84]. The authors synthesized MTNs by the controlled hydrolysis of titanium (IV) ethoxide in ethanol. The nanoparticles had an average diameter of

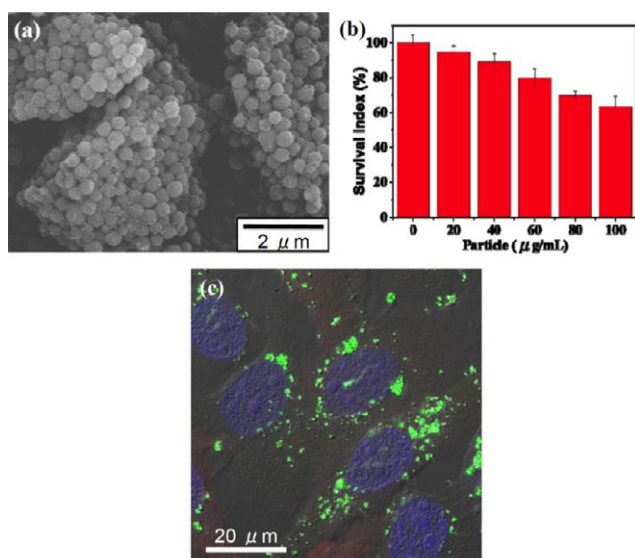


Figure 6. Characterization of MTNs. (a) SEM image of MTNs, indicating a uniform particle size of about 350 nm. (b) MTT assay of BT-20 cells treated with various concentrations of MTNs, showing good biocompatibility. (c) Merged fluorescence confocal image of flavin mononucleotide-MTNs (green dots) in BT-20 cancer cells where nuclei are stained with 4',6-diamidino-2-phenylindole (DAPI, blue spots) (reprinted with permission from [84] ©2011 RSC Publishing).

354 nm, a BET surface area of $237.3 \text{ m}^2 \text{ g}^{-1}$ and a pore size of about 2.8 nm. The viability test (MTT assay) in a human breast cancer cell line (BT-20) showed that MTNs have a good biocompatibility at concentrations as high as 0.4 g L^{-1} . To track the internalization *in vitro*, the authors took advantage of the strong interaction between titania and phosphate, and used a fluorescent probe flavin mononucleotide ($\lambda_{\text{ex}} = 460 \text{ nm}$; $\lambda_{\text{em}} = 530 \text{ nm}$). To evaluate the drug carrier properties of this platform, the authors loaded doxorubicin and monitored the release of the drug in solution and *in vitro*. The release of the drug was successfully observed *in vitro* by confocal microscopy. Moreover, the viability assay showed a decrease in proliferation after the cells have been incubated with doxorubicin-loaded MTNs. The authors demonstrated that MTNs could be an excellent drug delivery platform owing to their biocompatibility, ease of functionalization and high payload of therapeutic agents.

4. Conclusions

Mesoporous titania materials have been successfully applied in numerous fields. For photoelectronic applications, anatase-type crystalline mesoporous materials have been used in the photoelectrodes of DSSCs and as photocatalysts to solve global energy problems. Every application has its own requirement for the morphology of mesoporous titania. Therefore, the rational design and synthesis of mesoporous titania with controllable morphological and structural features are practically important. Research on the applications of mesoporous titania, such as sensing and drug delivery, is still in its early stages. We expect that more types of mesoporous

titania will be used in sensors and intracellular nanovehicles for biomedicine in the near future.

Acknowledgments

One of the authors (JLV-E) thanks the Carolina Postdoctoral Program for Faculty Diversity for a postdoctoral fellowship.

References

- [1] Yamauchi Y, Suzuki N, Radhakrishnan L and Wang L 2009 *Chem. Rec.* **9** 321
- [2] Kimura T and Kuroda K 2009 *Adv. Funct. Mater.* **19** 511
- [3] Ariga K 2004 *Chem. Rec.* **3** 297
- [4] Yanagisawa T, Shimizu T, Kuroda K and Kato C 1990 *Bull. Chem. Soc. Japan* **63** 988
- [5] Kresge C T, Leonowicz M E, Roth W J, Vartuli J C and Beck J S 1992 *Nature* **359** 710
- [6] Ni W B, Wang D C, Zhao Z Z, Huang Z J and Zhao J W 2010 *Chem. Lett.* **39** 98
- [7] Park J N, Shon J K, Jin M, Hwang S H, Park G O, Boo J H, Han T H and Kim J M 2010 *Chem. Lett.* **39** 493
- [8] Zeng T Y, Zhou Z M, Cheng Z M and Yuan W K 2010 *Chem. Lett.* **39** 680
- [9] Shirokura N, Nakajima K, Nakabayashi A, Lu D L, Hara M, Domen K, Tatsumi T and Kondo J N 2006 *Chem. Commun.* **2188**
- [10] Antonelli D M and Ying J Y 1995 *Angew. Chem., Int. Ed. Engl.* **34** 2014
- [11] Ulagappan N and Rao C N R 1996 *Chem. Commun.* **1685**
- [12] Froba M, Muth O and Reller A 1997 *Solid State Ionics* **101** 249
- [13] Niessen T E W, Niederer J P M, Gjeran T and Holderich W F 1998 *Microporous Mesoporous Mater.* **21** 67
- [14] Antonelli D M 1999 *Microporous Mesoporous Mater.* **30** 315
- [15] On D T 1999 *Langmuir* **15** 8561
- [16] Yang P D, Zhao D Y, Margolese D I, Chmelka B F and Stucky G D 1998 *Nature* **396** 152
- [17] Zheng J Y, Pang J B, Qiu K Y and Wei Y 2001 *J. Mater. Chem.* **11** 3367
- [18] Ogawa M 1996 *Chem. Commun.* **1149**
- [19] Ogawa M 1994 *J. Am. Chem. Soc.* **116** 7941
- [20] Yun H S, Miyazawa K, Zhou H S, Honma I and Kuwabara M 2001 *Adv. Mater.* **13** 1377
- [21] Grosso D, Soler-Illia G, Babonneau F, Sanchez C, Albouy P A, Brunet-Bruneau A and Balkenende A R 2001 *Adv. Mater.* **13** 1085
- [22] Smarsly B, Grosso D, Brezesinski T, Pinna N, Boissiere C, Antonietti M and Sanchez C 2004 *Chem. Mater.* **16** 2948
- [23] Wu C W, Ohsuna T, Kuwabara M and Kuroda K 2006 *J. Am. Chem. Soc.* **128** 4544
- [24] Nilsson E, Sakamoto Y and Palmqvist A E C 2011 *Chem. Mater.* **11** 2781
- [25] Carbajo M C, Enciso E and Torralvo M J 2007 *Colloids Surf. A* **293** 72
- [26] Ma T Y, Zhang X J and Yuan Z Y 2009 *Microporous Mesoporous Mater.* **123** 234
- [27] Wang L Z, Tomura S, Maeda M, Ohashi F, Inukai K and Suzuki M 2000 *Chem. Lett.* **1414**
- [28] Han S J, Choi S H, Kim S S, Cho M, Jang B, Kim D Y, Yoon J and Hyeon T 2005 *Small* **1** 812
- [29] Shibata H, Ogura T, Mukai T, Ohkubo T, Sakai H and Abe M 2005 *J. Am. Chem. Soc.* **127** 16396
- [30] Choi H, Stathatos E and Dionysiou D D 2006 *Thin Solid Films* **510** 107
- [31] Hafez H S 2009 *Mater. Lett.* **63** 1471
- [32] Tanaka S, Nogami D, Tsuda N and Miyake Y 2009 *J. Colloid Interface Sci.* **334** 188

- [33] Kim D S and Kwak S Y 2007 *Appl. Catal. A* **323** 110
- [34] Chen D, Huang F, Cheng Y B and Caruso R A 2009 *Adv. Mater.* **21** 2206
- [35] Guo C, Ge M, Liu L, Gao G, Feng Y and Wang Y 2010 *Environ. Sci. Technol.* **44** 419
- [36] Sun A, Li Z, Li M, Xu G, Li Y and Cui P 2010 *Powder Technol.* **201** 130
- [37] Chen D, Cao L, Huang F, Imperia P, Cheng Y B and Caruso R A 2010 *J. Am. Chem. Soc.* **132** 4438
- [38] Wang P, Teng S H and Tang F Q 2010 *Chem. Lett.* **39** 1140
- [39] Li H, Bian Z, Zhu J, Zhang D, Li G, Huo Y, Li H and Lu Y 2007 *J. Am. Chem. Soc.* **129** 8406
- [40] Ye M, Chen Z, Wang W, Shen J and Ma J 2010 *J. Hazard. Mater.* **184** 612
- [41] Wang Y Q, Tang X H, Yin L X, Huang W P, Hacoheh Y R and Gedanken A 2000 *Adv. Mater.* **12** 1183
- [42] Yu J C, Zhang L Z and Yu J G 2002 *New J. Chem.* **26** 416
- [43] Lu Y F, Fan H Y, Stump A, Ward T L, Rieker T and Brinker C J 1999 *Nature* **398** 223
- [44] Yamauchi Y, Takeuchi F, Todoroki S, Sakka Y and Inoue S 2008 *Chem. Lett.* **37** 72
- [45] Yamauchi Y and Kimura T 2008 *Chem. Lett.* **37** 892
- [46] Yamauchi Y, Suzuki N, Gupta P, Sato K, Fukata N, Murakami M, Shimizu T, Inoue S and Kimura T 2009 *Sci. Technol. Adv. Mater.* **10**
- [47] Yamauchi Y, Suzuki N, Sato K, Fukata N, Murakami M and Shimizu T 2009 *Bull. Chem. Soc. Japan* **82** 1039
- [48] Yamauchi Y, Gupta P, Sato K, Fukata N, Todoroki S I, Inoue S and Kishimoto S 2009 *J. Ceram. Soc. Japan* **117** 198
- [49] Kimura T, Kato K and Yamauchi Y 2009 *Chem. Commun.* **4938**
- [50] Oveisi H, Suzuki N, Beitollahi A and Yamauchi Y 2010 *J. Sol-Gel Sci. Technol.* **56** 212
- [51] Chen X and Mao S S 2007 *Chem. Rev.* **107** 2891
- [52] Fujishima A, Rao T N and Tryk D A 2000 *J. Photochem. Photobiol. C* **1** 1
- [53] Mills A and LeHunte S 1997 *J. Photochem. Photobiol. A* **108** 1
- [54] Hoffmann M R, Martin S T, Choi W Y and Bahnemann D W 1995 *Chem. Rev.* **95** 69
- [55] Linden M, Blanchard J, Schacht S, Schunk S A and Schüth F 1999 *Chem. Mater.* **11** 3002
- [56] Peng T Y, Zhao D, Dai K, Shi W and Hirao K 2005 *J. Phys. Chem. B* **109** 4947
- [57] Peng T Y, Zhao D, Song H B and Yan C H 2005 *J. Mol. Catal. A: Chem.* **238** 119
- [58] Xiao J R, Peng T Y, Li R, Peng Z H and Yan C H 2006 *J. Solid State Chem.* **179** 1161
- [59] Dai K, Peng T, Chen H, Liu J and Zan L 2009 *Environ. Sci. Technol.* **43** 1540
- [60] Li D L, Zhou H S and Honma I 2004 *Nat. Mater.* **3** 65
- [61] Oveisi H, Beitollahi A, Jiang X, Sato K, Nemoto Y, Fukata N and Yamauchi Y 2011 *J. Nanosci. Nanotechnol.* at press
- [62] Oveisi H, Jiang X F, Nemoto Y, Beitollahi A and Yamauchi Y 2011 *Microporous Mesoporous Mater.* **139** 38
- [63] Oveisi H, Beitollahi A, Imura M, Wu C W and Yamauchi Y 2010 *Microporous Mesoporous Mater.* **134** 150
- [64] Zhou W, Sun F, Pan K, Tian G, Jiang B, Ren Z, Tian C and Fu H 2011 *Adv. Funct. Mater.* **21** 1922
- [65] Oveisi H, Rahighi S, Jiang X, Agawa Y, Beitollahi A, Wakatsuki S and Yamauchi Y 2011 *Chem. Lett.* **40** 420
- [66] Oveisi H, Rahighi S, Jiang X, Nemoto Y, Beitollahi A, Wakatsuki S and Yamauchi Y 2010 *Chem. Asian J.* **5** 1978
- [67] Hu X, Li G and Yu J C 2010 *Langmuir* **26** 3031
- [68] Gratzel M 2001 *Nature* **414** 338
- [69] Gratzel M 2001 *J. Sol-Gel Sci. Technol.* **22** 7
- [70] Gratzel M 2003 *J. Photochem. Photobiol. C* **4** 145
- [71] Gratzel M 2004 *J. Photochem. Photobiol. A* **168** 235
- [72] Oregan B and Gratzel M 1991 *Nature* **353** 737
- [73] Uchida S, Chiba R, Tomiha M, Masaki N and Shirai M 2002 *Electrochemistry* **70** 418
- [74] Adachi M, Murata Y, Takao J, Jiu J T, Sakamoto M and Wang F M 2004 *J. Am. Chem. Soc.* **126** 14943
- [75] Song M Y, Kim D K, Ihn K J, Jo S M and Kim D Y 2004 *Nanotechnology* **15** 1861
- [76] Khan M A, Akhtar M S and Yang O B 2010 *Sol. Energy* **84** 2195
- [77] Zhao D, Peng T, Lu L, Cai P, Jiang P and Bian Z 2008 *J. Phys. Chem. C* **112** 8486
- [78] Nazeeruddin M K, Kay A, Rodicio I, Humphrybaker R, Muller E, Liska P, Vlachopoulos N and Gratzel M 1993 *J. Am. Chem. Soc.* **115** 6382
- [79] Peng T, Fan K, Zhao D and Chen J 2010 *J. Phys. Chem. C* **114** 22346
- [80] Patra A K, Das S K and Bhaumik A 2011 *J. Mater. Chem.* **21** 3925
- [81] Chen H W, Liang C P, Huang H S, Chen J G, Vittal R, Lin C Y, Wu K C W and Ho K C 2011 *Chem. Commun.* **47** 8346
- [82] Devi G S, Hyodo T, Shimizu Y and Egashira M 2002 *Sensors Actuators B* **87** 122
- [83] Benkstein K D and Semancik S 2006 *Sensors Actuators B* **113** 445
- [84] Wu K C W, Yamauchi Y, Hong C Y, Yang Y H, Liang Y H, Funatsu T and Tsunoda M 2011 *Chem. Commun.* **47** 5232